Chalmers Publication Library


This paper is a postprint of a paper submitted to and accepted for publication in IET Microwaves, Antennas & Propagation and is subject to Institution of Engineering and Technology Copyright. The copy of record is available at **IET Digital Library.**

Yang, J. (2012) Periodicity of the input impedance of log-periodic array antennas. *IET Microwaves, Antennas & Propagation*, vol. 6, no. 10, pp. 1117-1122.

http://dx.doi.org/10.1049/iet-map.2011.0599

(Article begins on next page)

# On Periodicity of the Input Impedance of Log-periodic Array Antennas

Jian Yang

Dept. of Signals and Systems, Chalmers Univ. of Technology,

41296 Gothenburg, Sweden.

February 21, 2012

**Abstract**

One way for an antenna to achieve an ultra-wideband (UWB) performance is to employ a log-periodic array (LPA), which usually involves many scaled elements cascaded one after another. If a LPA is infinite at both ends (infinitely small at one end and extended to infinitely large at the other end), it is obvious that the input impedance of the array is periodical over frequencies. However, for practical antennas, infinite LPAs have to be truncated. The purely periodical performance will not hold anymore. On the other hand, UWB log-periodic array antennas are often very large in terms of the wavelength at the highest operating frequency, which makes numerical simulation very time consuming. We present a theoretical analysis of the periodicity of the input impedance of a general finite LPA. New periodicity formulas are verified by examples of the Eleven antenna - a folded dipole LPA, with simulated and measured data. By using the new periodicity formula, the input impedance of a large LPA antenna at high frequencies can be predicted by its values at low frequencies, which leads to an efficient calculation when a numerical simulation is employed, and helps to have an efficient design of large LPA antennas.

**Keywords:** periodicity, log-periodic antenna, ultra-wideband antenna, input impedance, Eleven antenna

# 1 Introduction

Log-periodic array (LPA) antennas have been widely used in wideband applications since the first one was introduced 50 years ago [1–3]. They can provide a constant radiation function and a low reflection coefficient over a wide frequency band, which are demanded in many applications.

Recent developments on LPA antennas can be summarized by the representatively selected literatures of [4–12], where different LPA antennas have been investigated for different applications. Particularly, the next generation of ultra-wideband (UWB) radio telescopes has drawn a lot of attention for extensive research on UWB antennas [13], such as in the Square Kilometer Array (SKA) and the Very Long Baseline Interferometry 2010 (VLBL2010) projects.

A new decade bandwidth feed for reflector antennas, the Eleven feed [11], has been developed during recent years at Chalmers University of Technology. The Eleven feed is a cascaded log-periodic folded dipole array, having a nearly constant beamwidth with about 11 dBi directivity, a fixed phase center location, and a simple geometry of a low profile.

Although LPA antennas have been investigated intensively, some new questions still arise. For example, if a LPA is infinite at both ends, infinitely small at one end and extended to infinitely large at the other end, it is obvious that both the radiation function and the input impedance are periodical over frequencies. However, in practice, infinite LPAs have to be truncated at both ends. The pure periodicity of the performance does not hold anymore. On the other hand, the size of most LPAs is quite large in terms of the wavelength at the highest operating frequency. A large computation time is therefore needed for obtaining the performance when a numerical method is employed.

The purpose of this paper is to derive a new formula of the periodicity for the input impedance of a general finite LPA antenna. By applying this formula, the input impedance of a large LPA antenna at high frequencies can be calculated by its values at low frequencies. When a numerical approach is employed, this leads to a very efficient impedance calculation, because the size of a

LPA in terms of the wavelength is smaller at a low frequency than that at a high frequency.

In the paper, the theoretical derivation of the periodicity formula is presented in Section II. Then, an extension of this theorem is derived in Section III. Two examples are presented in Section IV with simulated and measured data for verifying the theoretical analysis.

# 2 Periodicity of the Input Impedance

Without loss of generality, the diagram in Fig. 1 is used to represent an N-element cascaded log-periodic array (LPA), where the dipole symbols indicate the radiation from elements. In the analysis here, it is assumed that the excitation (feeding) port is at the smallest radiation element of the array, which is also the case in the most LPAs in practice.

## 2.1 Three State Regions

In general, LPA antennas have three state regions [14] (transmission-line, active and stop) over their operating frequency band. We define the three regions in a stricter way than that in [14] for the sake of the analysis here.

*1) The transmission-line region* at frequency $f$ is such a region where the elements do not radiate. This is because the size of the elements is much smaller than the wavelength at $f$, and therefore the elements function as a transmission line.

Since there is no radiation from the elements in this region, no mutual couplings exist between them and the rest elements in the LPA. Therefore, the total ABCD matrix of this region can be obtained by multiplication of all ABCD matrices of each element in the region. Referring to Fig. 1, the total ABCD matrix $\mathbf{T}_{trans}$ of the transmission-line region at frequency $f$, including elements from 1 to $L$, can be expressed by

$$\mathbf{T}_{trans}(f) = \prod_{i=1}^{L} \mathbf{T}_i(f)\,, \tag{1}$$

where $\mathbf{T}_i(f), (i = 1, \cdots, L)$ is the ABCD matrix of the $i$th element in the LPA.

*2) The active region* at frequency $f$ is such a region where the elements radiate. Referring to

Fig. 1, the active region includes elements from $L+1$ to $M$. Since there are radiation from these elements and therefore mutual couplings among them, we can not simply multiply all element ABCD matrices in this region to obtain the total ABCD matrix of the region.

*3) The stop region* at frequency $f$ is the region after the active region, where there is no radiation from the elements due to the null currents on the elements. The null currents on the elements in the stop region are the result of the following fact. The current passed through the previous element and the current induced by mutual couplings from the active elements are of the same amplitude and 180° out of phase, as depicted in Fig. 2. In an ideal case, the current on the elements in the stop region vanishes. More realistically in practice, the level of the element current in the region is low. Referring to Fig. 1, we have

$$I_i(f) \approx 0, i \geq M+1\,. \tag{2}$$

It should be noted that not all LPAs have the three regions. The configuration of the radiation elements in a LPA should satisfy certain conditions to have the three regions [15]. Most LPAs in practice satisfy the conditions. For the analysis in the paper, we assume that the LPA has these three regions.

## 2.2 Properties and Theorem

When a LPA has the above-defined three regions, we have the following properties and theorem.

**Property I** If elements $i$ and $i+1$ are in the transmission-line region, due to the log-periodic scaling of the geometry, we have

$$\mathbf{T}_{i+1}(f/k) = \mathbf{T}_i(f), \tag{3}$$

where $k$ is the scaling factor of the LPA. Therefore, we have

$$\mathbf{T}_{i+1}(f/k^i) = \mathbf{T}_1(f). \tag{4}$$

**Property II** If the active region at frequency $f$ includes elements from $L+1$ to $M$, then the active region at frequency $f/k$ will include elements from $L+2$ to $M+1$ due to the log-periodic

scaling of the geometry. From this geometry scaling and the fact that the stop region does not affect the currents on the elements in the active region, we have

$$Z_{in,L+2}(f/k) = Z_{in,L+1}(f) \tag{5}$$

where $Z_{in,L+2}$ and $Z_{in,L+1}$ are the input impedance at input ports of element $L+2$ and $L+1$, respectively.

**Theorem** Assume that a LPA antenna has an operating frequency band from $f_{low}$ to $f_{high}$, and in this frequency band there always exist the above-defined three regions. Then, if frequencies $f$ and $f/k^n$ are both in the frequency band, we have

$$Z_{in}(f/k^n) = \mathbf{T}^{(n)}(f,k) \oplus Z_{in}(f) \tag{6}$$

where

$$\mathbf{T}^{(n)}(f,k) = \begin{bmatrix} A^{(n)} & B^{(n)} \\ C^{(n)} & D^{(n)} \end{bmatrix} = \prod_{i=0}^{n-1} \mathbf{T}_1(f/k^{n-i}) \tag{7}$$

and operation $\oplus$ means that

$$\mathbf{T}^{(n)}(f,k) \oplus Z_{in}(f) = \frac{A^{(n)} \cdot Z_{in}(f) + B^{(n)}}{C^{(n)} \cdot Z_{in}(f) + D^{(n)}} \tag{8}$$

***Proof*** Referring to Fig. 1, the transmission-line region includes elements from 1 to $L$ at frequency $f$. Then, we have

$$\begin{bmatrix} V_1(f) \\ I_1(f) \end{bmatrix} = \prod_{i=1}^{L} \mathbf{T}_i(f) \begin{bmatrix} V_{L+1}(f) \\ I_{L+1}(f) \end{bmatrix} \tag{9}$$

From (9), we can obtain the relation between the input impedance of the array $Z_{in} = V_1/I_1$ and the input impedance at the port of the active region $Z_{in,L+1} = V_{L+1}/I_{L+1}$ as

$$Z_{in}(f) = \prod_{i=1}^{L} \mathbf{T}_i(f) \oplus Z_{in,L+1}(f)\,. \tag{10}$$

At frequency $f/k$, the transmission-line region therefore includes elements from 1 to $L+1$, and we have

$$\begin{aligned}\begin{bmatrix} V_1(f/k) \\ I_1(f/k) \end{bmatrix} &= \prod_{i=1}^{L+1} \mathbf{T}_i(f/k) \begin{bmatrix} V_{L+2}(f/k) \\ I_{L+2}(f/k) \end{bmatrix} \\ &\overset{by(3)}{=} \mathbf{T}_1(f/k) \prod_{i=1}^{L} \mathbf{T}_i(f) \begin{bmatrix} V_{L+2}(f/k) \\ I_{L+2}(f/k) \end{bmatrix}.\end{aligned} \tag{11}$$

From the above, we can obtain

$$\begin{aligned}Z_{in}(f/k) &= \mathbf{T}_1(f/k) \prod_{i=1}^{L} \mathbf{T}_i(f) \oplus Z_{in,L+2}(f/k) \\ &\overset{by(5)}{=} \mathbf{T}_1(f/k) \prod_{i=1}^{L} \mathbf{T}_i(f) \oplus Z_{in,L+1}(f) \\ &\overset{by(10)}{=} \mathbf{T}_1(f/k) \oplus Z_{in}(f)\end{aligned} \tag{12}$$

By the same procedure, we have

$$\begin{aligned}Z_{in}(f/k^n) &= \prod_{i=0}^{n-1} \mathbf{T}_1(f/k^{n-i}) \oplus Z_{in}(f) \\ &= \mathbf{T}^{(n)}(f,k) \oplus Z_{in}(f)\end{aligned} \tag{13}$$

**Variation of the Theorem** We can re-write the theorem in (6) as follows

$$Z_{in}(f) = \mathbf{T}^{(n)}(f,k) \ominus Z_{in}(f/k^n) \tag{14}$$

where $\mathbf{T}^{(n)}(f,k)$ is the same as defined in (7) and operation $\ominus$ means that

$$\mathbf{T}^{(n)}(f,k) \ominus Z_{in}(f/k^n) = \frac{D^{(n)} \cdot Z_{in}(f/k^n) - B^{(n)}}{A^{(n)} - C^{(n)} \cdot Z_{in}(f/k^n)}. \tag{15}$$

The above formula states that the input impedance of a LPA at a high frequency can be calculated by its value at a low frequency and the ABCD matrix of the first element over a band from the low frequency to the high frequency. When we use a numerical electromagnetic solver to obtain the input impedance of a large LPA over a wide frequency band, we need only simulate 1) the whole geometry of the LPA antenna up to a much lower frequency than the highest operating frequency (for example, the one third of the highest frequency), and 2) a

simple geometry which includes only the first element over the whole frequency band, instead of simulating the whole geometry over the whole band (often large computation time). Therefore, the theorem in (14) provides an efficient calculation.

## 3 Extension of the Periodicity Theorem

In practice, there are always feeding networks or other circuits that are not of log-periodic structure connected to LPA antennas, as show in Fig. 3. We use $\mathbf{T}_0(f)$ to represent a feeding network as

$$\mathbf{T}_0 = \begin{bmatrix} A_0 & B_0 \\ C_0 & D_0 \end{bmatrix} \tag{16}$$

Then, the total input impedance at the feeding port $p_0$ can be expressed as

$$\begin{aligned} Z_{in0}(f) &= \mathbf{T}_0(f) \oplus Z_{in}(f) \\ &= \mathbf{T}_0(f) \oplus \{\mathbf{T}^{(n)}(f,k) \ominus Z_{in}(f/k^n)\}\,. \end{aligned} \tag{17}$$

This states that in order to obtain the input impedance of a LPA antenna with a feeding network, instead of simulating the whole structure over the whole band of $(f_{low}, f_{high})$, we can simulate the following three parts, as shown in Fig. 3: 1) only the feeding network over the whole band of $(f_{low}, f_{high})$; 2) only the first element of the LPA over the whole band of $(f_{low}, f_{high})$; and 3) the whole log-periodic structure over the band of $(f_{low}, f_1)$, where $f_1 \ll f_{high}$ (e.g. $f_1 \leq f_{high}/3$). Then, by using (17), we can calculate the input impedance of the whole LPA antenna over the whole band efficiently.

The criterion of choosing $f_1$ is that the element with the operating frequency of $f_1$ should have at least 5-element spacing to the low-frequency-end board of the array, such as the case in the paper.

## 4 Examples

Two examples of the Eleven antenna are presented here to verify the analysis in Sects. 2

and 3. The basic geometry of the Eleven antenna is two parallel dipoles separated by half wavelength over a ground plane, referred to as the 11 configuration and the reason for the name of the antenna.

For convenience, the reflection coefficient $\Gamma$ is used for the verification, instead of using the input impedance $Z_{in}$, with the relation between them as

$$\Gamma(f) = \frac{Z_{in}(f) - Z_0}{Z_{in}(f) + Z_0}, \tag{18}$$

where $Z_0$ is the characteristic impedance of the transmission line at the input port.

### 4.1 Simulation of a 14-pair-folded-dipole Eleven antenna without feeding network

Fig. 4 shows the configuration of a 14-pair folded-dipole Eleven antenna, modeled in CST Microwave Studio [16]. Referring to Fig. 5(a), the definition of the different dimensions can be obtained by corresponding data in both Table 1 and Fig. 5(a).

The S matrix of a single folded dipole can be obtained analytically [17]. However, for simplicity and convenience, the numerically simulated results are used here. Fig. 5(b) shows the simulated S parameters of the first folded dipole of the array. It can be seen that the first folded dipole functions as an almost perfect transmission line up to 6 GHz (very low reflection coefficient and almost 0 dB transmission coefficient). Above 6 GHz, it starts radiating gradually. But up to 15 GHz, the transmission loss of the first folded dipole is still better than $-0.5$ dB, which means that the dipole can still be considered as a good transmission line up to 15 GHz.

Fig. 6 shows the simulated and calculated results of the reflection coefficient of the Eleven antenna with the port impedance of $Z_0 = 200$ Ohm by the following two methods: 1) CST full simulation of the whole geometry over 2–18 GHz (solid line); 2) CST simulations of the whole geometry over 2–4.8 GHz and only the first dipole over 2–18 GHz, and then using (14) and (18) to predict the reflection coefficient over 4.8–18 GHz (dash line). It can be seen that the agreement between these two methods is very good up to 15 GHz. The average error of the

peak values (11 peaks from 4.8 to 16 GHz) is about 1.6%. At the frequencies above 15 GHz, the discrepancy starts to increase, since the first dipoles starts to radiate, not as a transmission line anymore at these high frequencies.

It took 41266 seconds ($11h27m46s$) by the first method (full CST simulation) and 6318 seconds ($1h45m9s$) by the second method (using the new periodicity theorem) on a same PC (AMD Athlon dual core Processor 4400, 2.3 GHz, 4.00GB RAM). The computational efficiency has been increased more than 6 times by using the new periodicity theorem.

### 4.2 Simulation and measurement of a 1–10 GHz Eleven antenna with feeding network

The 1–10 GHz linearly polarized Eleven antenna, made of metal strips on a thin Kevlar sheet and supported by a foam structure, was reported in [8] and is shown here in Fig. 7. Its dimensions can be found in [8].

The antenna consists of a simple center feeding network (non log-periodic structure, see the CST modeling shown in Fig. 8) and a pair of 21-folded-dipole log-periodic arrays. The first two folded dipoles were designed by different parameters from the rest 19 dipoles, which makes these two dipoles a non log-periodic structure compared to the rest 19 dipoles (Fig. 8(a)). Therefore, we include these two dipoles in the non log-periodic feeding network shown in Fig. 8(b). The port definitions are shown in Fig. 8(c), where the center dielectric cylinder and the ground plane are hidden for clarity. The port impedance $Z_0$ is 100 Ohm at port 1, and 200 Ohm at port 2. A symmetry plane of perfect magnetic conductor (PMC) is employed in $y$-$z$ plane in the modeling.

Since the metal strips and the Kevlar sheet are very thin ($35\mu m$ and $20\mu m$ thick, respectively), we can assume that they have infinitely thin thickness. The relative permittivity of the foam is very close to 1, so its effect is negligible. Therefore, the rest 19-folded-dipole-pair LPA is a purely log-periodic structure.

The reflection coefficient of the antenna is obtained by using the new periodicity theorem in

the following steps.

1) CST simulation of the feeding network including the two first dipoles over 1–13 GHz to get $T_0(f)$. Fig. 9 shows the simulated magnitudes of the S parameters of this feeding network.

2) CST simulation of the third dipole of the LPA over 1–13 GHz to obtain $T^n(f,k)$ . Fig. 10 shows the simulated magnitudes of the S parameters, where we can see that this dipole functions as a good transmission line up to 10 GHz.

3) CST simulation of the pure LPA (from dipole 3 to 21) only over 1–4.3 GHz.

4) Using (17) and (18) to calculate the reflection coefficient over 4.3–13 GHz (the dash line in Fig. 11).

Fig. 11 shows the result of the present method (the dash line), together with the measurement data (dot line) and the full CST simulation data of the whole geometry over 1–13 GHz. The average error of the peak values (10 peaks from 4.3 to 12 GHz) is about 2.7%. It took 19234 seconds ($5h20m34s$) by the full CST simulation and 3505 seconds ($0h58m5s$) by using the new periodicity theorem on a same PC (AMD Athlon dual core Processor 4400, 2.3 GHz, 4.00GB RAM). The computation time for the present method is less than one fifth of the time for the full CST simulation. It can be seen that the present method by applying the new periodicity formula can predict the input impedance of a large LPA antenna accurately and efficiently.

It should be noted that the present method gives an efficient calculation of the input impedance when a numerical simulation is involved, not only for CST MWS.

## 5 Conclusion

In the paper, a new periodicity theorem for the input impedance of a general large log-periodic array (LPA) antenna has been derived. By using this theorem, the input impedance of a large LPA antenna can be obtained very efficiently when a numerical simulation is involved, such as more than 5-6 times faster computations for the cases in the paper.

## Acknowledgment

This work has been supported in part by The Swedish Foundation for Strategic Research (SSF) within the Strategic Research Center Charmant.

## References


[1] Isbell, D. E.: 'Log periodic dipole array', IRE Trans. Antennas Propogat., 1960, **8**, (3), pp. 260-267

[2] Carrel, R.: 'The design of log-periodic dipole antennas', IRE Int. Conv. Rec., 1961, **9**, (1), pp. 61-75

[3] Vito, G. D. and Stracca, G. B.: 'Comments on the design of log-periodic dipole antennas', IEEE Trans. Antennas Propogat., 1973, **21**, (3), pp. 303-308

[4] Olsson, R., Kildal, P.-S. and Weinreb, S.: 'The Eleven antenna: a compact low-profile decade bandwidth dual polarized feed for reflector antennas', IEEE Trans. on Antennas Propagat., 2006, **54**, (2), pp. 368-375

[5] Kim, S. H., Choi, J. H., Baik, J. W. and Kim, Y. S.: 'CPW-fed log-periodic dumb-bell slot antenna array', Electronics Lett., 2006, **42**, (8), pp. 436-438

[6] Aghdam, K., Faraji-Dana, R. and Rashed-Mohassel, J.: 'Compact dual-polarisation planar log-periodic antennas with integrated feed circuit', IEE Proceedings H – Microwaves, Antennas and Propagation, 2005, **152**, (5), pp. 359-366

[7] Hall, P.: 'Multioctave bandwidth log-periodic microstrip antenna array', IEE Proceedings H – Microwaves, Antennas and Propagation, 1986, **133**, (2), pp. 127-136

[8] Yang, J., Chen, X., Wadefalk, N. and Kildal, P.-S.: 'Design and realization of a linearly polarized Eleven feed for 1–10 GHz', IEEE Antennas Wireless Propag. Lett., 2009, **8**, (1), pp. 64-68

[9] Hamid, M. R., Hall, P. S. and Gardner, P.: 'Frequency reconfigurable log periodic patch array', Electronics Lett., 2010, **46**, (25), pp. 1648-1650

[10] Zhai, G. H., Hong, W., Wu, K. and Kuai, Z. Q.: 'Wideband substrate integrated printed log-periodic dipole array antenna', IET Microwaves Antennas Propagat., 2010, **4**, (7), pp. 61-75

[11] Yang, J., Pantaleev, M., Kildal, P.-S., Klein, B., Karadikar, Y., Helldner, L., Wadefalk, N. and Beaudoin, C.: 'Cryogenic 2-13 GHz Eleven feed for reflector antennas in future wideband radio telescopes', IEEE Trans. Antennas Propagat., 2011, **59**, (6), pp. 1918-1934

[12] Yang, J., Pantaleev, M., Kildal, P.-S. and Helldner, L.: 'Design of compact dual-polarized 1.2–10 GHz Eleven feed for decade bandwidth radio telescopes', IEEE Trans. Antennas Propagat., 2012, **60**, to appear

[13] The Special Issue on Antennas for Next Generation Radio Telescopes, IEEE Trans. Antennas Propagat., 2011, **59**, (6)

[14] Kraus, J. D. and Marhefka, R. J.: 'Antennas For All Applications' (Springer, 2003)

[15] Yang, J.: 'On conditions for constant radiation characteristics for log-periodic array antennas', IEEE Trans. Antennas Propagat., 2010, **58**, (5), pp. 1521-1526

[16] CST Microwave Studio; http://www.cst.com.

[17] Yang, J., Nyberg, D., and Yin, J.: 'Impedance matrix of a folded dipole pair under eleven configuration', IET Microwaves Antennas Propagat., 2010, **4**, (6), pp. 697-703

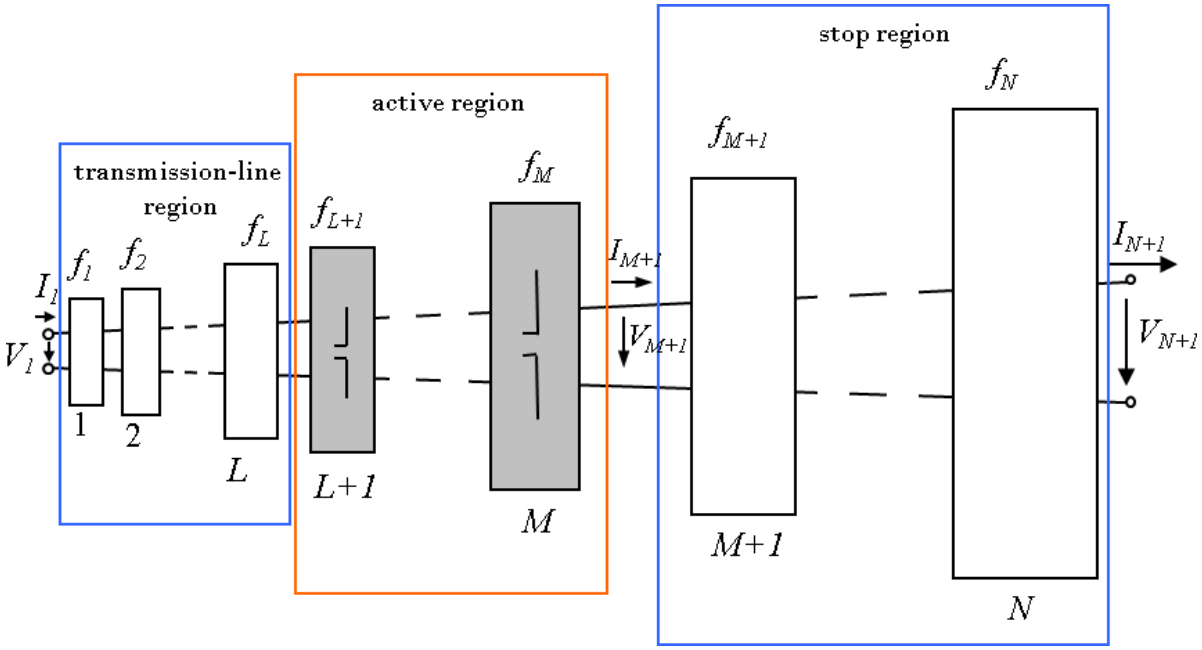


Figure 1: Block diagram presentation of a general N-element cascaded log-periodic array. $V_i$ and $I_i$ $(i = 1, \cdots, N+1)$ are port voltages and currents.

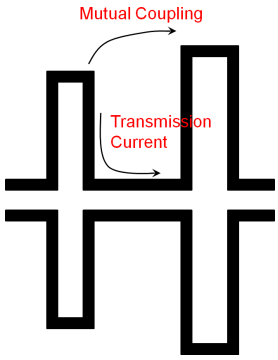


Figure 2: Transmission current and induced current due to mutual couplings.

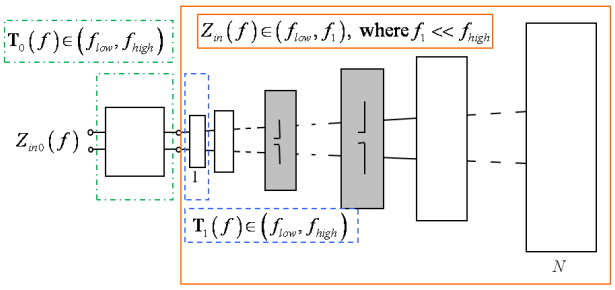


Figure 3: Diagram of LPA antenna with a feeding network.

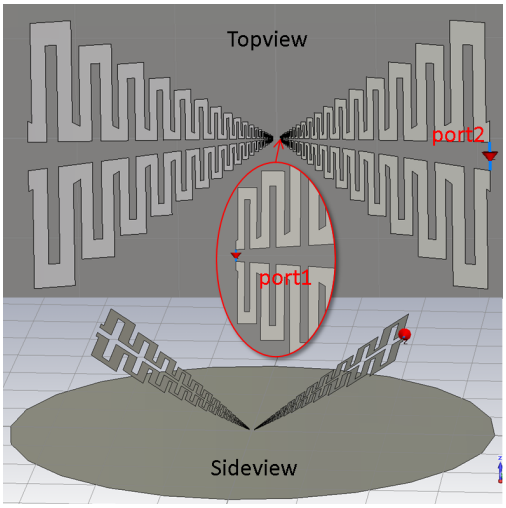


Figure 4: Configuration of the 14-pair Eleven antenna.

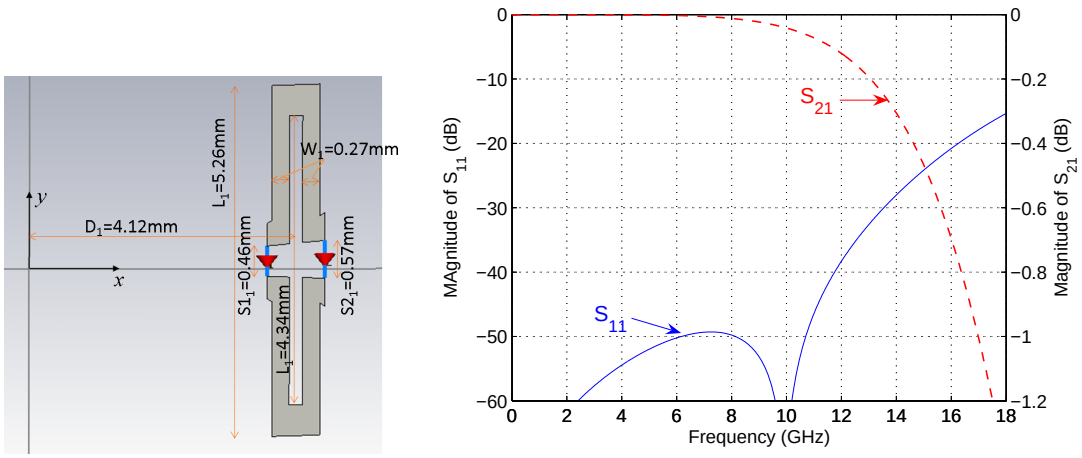


(a) Definition of dimensions

(b) Simulated data

Figure 5: CST simulated S parameters of the first folded dipole in the 14-pair Eleven antenna.

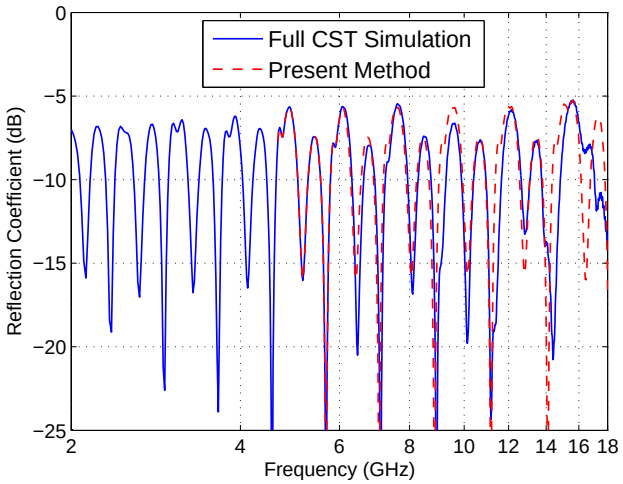


Figure 6: Simulated and calculated reflection coefficient of the 14-pair Eleven antenna.

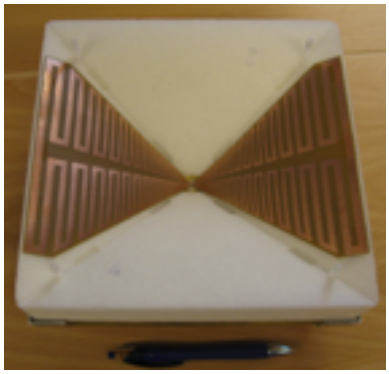

Figure 7: The prototype of 1–10 GHz linearly polarized Eleven antenna.

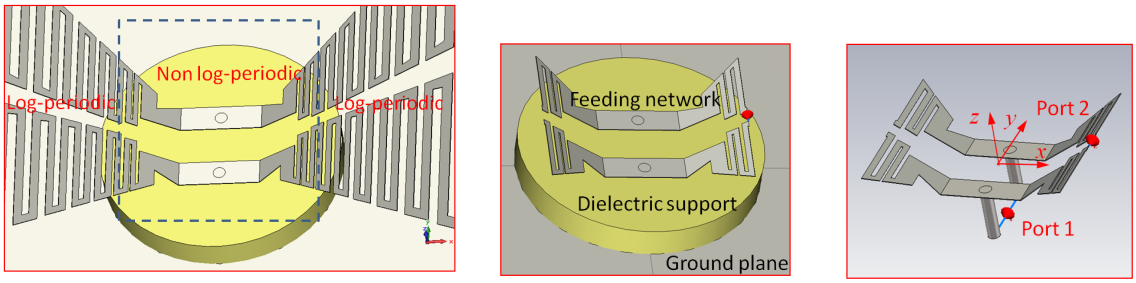


(a) Center part (b) Feeding network (c) Port definitions

Figure 8: The feeding network of the 1–10 GHz Eleven feed modeled in CST MWS, which includes the first two non log-periodic dipoles.

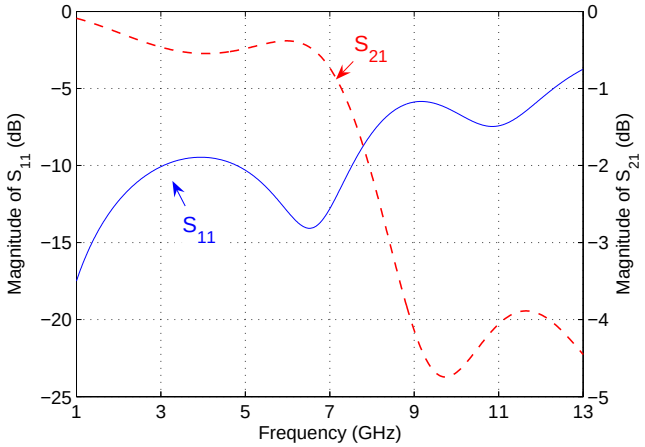


Figure 9: Simulated S parameters of the feeding network of the 1–10 GHz Eleven antenna.

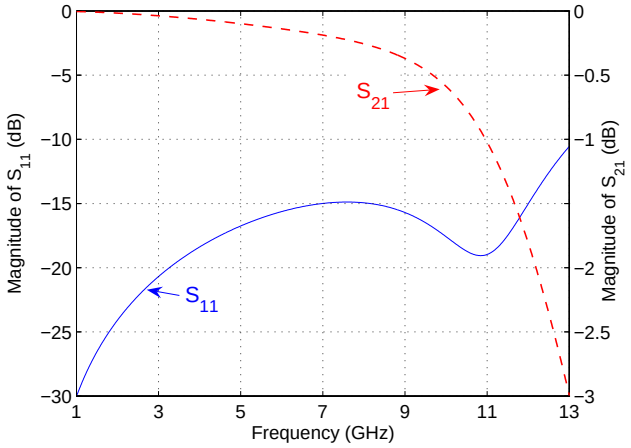


Figure 10: Simulated S parameters of the third dipole of the 1–10 GHz Eleven antenna.

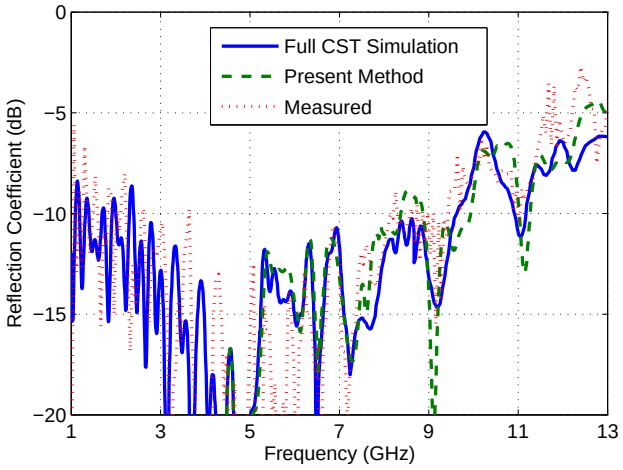


Figure 11: Measured and calculated reflection coefficient of the linearly polarized 1–10 GHz Eleven antenna including the feeding network.

Table 1: Dimensions of dipole $i$ ($i = 1, \cdots, 14$) of the 14-pair folded-dipole array with a scaling factor $k$

| $L_i$ (mm) | $l_i$ (mm) | $W_i$ (mm) | $S1_i$ (mm) |
|---|---|---|---|
| $5.26 \cdot k^{i-1}$ | $4.34 \cdot k^{i-1}$ | $0.27 \cdot k^{i-1}$ | $0.46 \cdot k^{i-1}$ |
| $S2_i$ (mm) | $h_i$ (mm) | $D_i$ (mm) | $k$ |
| $0.57 \cdot k^{i-1}$ | $13.3 \cdot k^{i-1}$ | $4.12 \cdot k^{i-1}$ | 1.24 |